

## **Quantitative 2D J-resolved metabolite-cycled semiLASER spectroscopy of metabolites and macromolecules in the human brain at 9.4 T**

Saipavitra Murali-Manohar<sup>1,2,3,4\*</sup>, Tamas Borbath<sup>1,2</sup>, Andrew Martin Wright<sup>1,5,6</sup>, Nikolai I. Avdievich<sup>1</sup>, and Anke Henning<sup>1,6</sup>

<sup>1</sup> High-Field Magnetic Resonance, Max Planck Institute for Biological Cybernetics, Tübingen, Germany

<sup>2</sup> Faculty of Science, University of Tübingen, Tübingen, Germany

<sup>3</sup> The Russell H. Morgan Department of Radiology and Radiological Science, Johns Hopkins University School of Medicine, Baltimore, MD, United States of America

<sup>4</sup> F.M. Kirby Research Center for Functional Brain Imaging, Kennedy Krieger Institute, Baltimore, MD, United States of America

<sup>5</sup> IMPRS for Cognitive & Systems Neuroscience, Tübingen, Germany

<sup>6</sup> Advanced Imaging Research Center, UT Southwestern Medical Center, Dallas, Texas

**Grant sponsors:** This project was co-sponsored by the Horizon 2020/ CDS-QUAMRI Grant number: 634541 (A. Henning, T. Borbath, and S. Murali-Manohar), SYNAPLAST Grant number: 679927 (A. Henning, A.M. Wright, and S. Murali-Manohar), and Cancer Prevention and Research Institute of Texas (CPRIT) Grant number: RR180056 (A. Henning).

Words total: 4391

\*Correspondence to Saipavitra Murali-Manohar PhD., The Russell H. Morgan Department of Radiology and Radiological Science, Johns Hopkins University School of Medicine, Baltimore, MD, USA.

E-mail: [svenka23@jhmi.edu](mailto:svenka23@jhmi.edu)

## Abstract

### Purpose:

While two-dimensional (2D) in vivo spectroscopy yields rich information and has been successfully used in clinical trials, it requires a localization scheme that minimizes the impact of chemical shift displacement on J-coupling evolution, a robust frequency drift correction and dedicated processing and quantification methods. Considering these needs this study demonstrates a novel data acquisition and an analysis pipeline to quantify 16 metabolites in mmol/kg in the human brain using a 2D J-resolved metabolite-cycled (MC) semiLASER localization sequence at 9.4 T in the human brain.

### Methods:

Metabolite spectra were acquired in vivo using the newly developed J-resolved MC semiLASER localization sequence with maximum echo sampling (MES) at 9.4 T. In order to account for the underlying macromolecular (MM) spectra in the acquired metabolite spectra, J-resolved MM spectra were acquired using a double inversion recovery (DIR) J-resolved MC semiLASER. Spectral fitting was performed with ProFit 2.0 using a simulated basis set from VesPA tailored to 2D J-resolved semiLASER with MES. Finally, metabolite concentrations were calculated using internal water referencing.

### Results:

Tissue concentrations for 16 metabolites in mmol/kg are reported after correcting for number of protons, tissue content, and relaxation effects of both water and metabolites at 9.4T. Quantification results of spectra considering 8 and 2 averages per TE did not show any significant differences.

### Conclusion:

2D spectra of metabolites acquired at 9.4T and 2D MMs acquired at any field strength are presented for the first time. Basis set simulation and quantification of metabolites for metabolite spectra acquired using maximum-echo-sampled 2D J-resolved semiLASER was performed for the first time. The sensitivity in the detection of J-coupled metabolites such as glutamine, glucose or lactate. At ultra-high field, the acquisition duration of 2D MRS can be also substantially reduced since only a very low number of averages per TE are needed.

**Keywords:** 2D J-resolved spectroscopy, Ultra-high field, Maximum echo sampling, ProFit 2.0, Quantification, semiLASER, Metabolite-cycling

**Abbreviations:** UHF, ultra-high field; NMR, nuclear magnetic resonance; 2D, two-dimensional; MRS, magnetic resonance spectroscopy, <sup>1</sup>H, proton; DIR, double inversion recovery; MES, maximum echo sampling; SAR, specific absorption rate; SNR, signal-to-noise ratio; MC, metabolite-cycling; MM, mobile macromolecule.

## 1. Introduction

Single voxel proton magnetic resonance spectroscopy (<sup>1</sup>H-MRS) is a popular non-invasive technique used to study the metabolism in the human brain. It enables detection and quantification of the neurochemical profile in a particular region of interest, thereby aiding

detection of various pathologies in the human brain<sup>1</sup>. However, complex spectral patterns and severe spectral overlap often pose a challenge in quantifying individual metabolite concentrations<sup>2</sup>. Therefore, enhancing the signal-to-noise ratio (SNR) and spectral resolution has always been one of the main aims of the MRS community.

One technique used by the NMR community to reduce spectral overlap is multi-dimensional spectroscopy<sup>3,4</sup>. Homonuclear two-dimensional (2D) techniques such as correlation spectroscopy and J-resolved spectroscopy were shown to be feasible in vivo at 1.5, 3 and 7 T<sup>5-7</sup> and hold the promise to yield accurate quantification results for a large number of metabolites in clinical trials of neurological and psychiatric disorders<sup>8-14</sup>. Nevertheless, at clinical field strength this technique owes to longer measurement durations than 1D MRS with 4 to 8 averages needed for each encoding step and requires non-standard pre-processing, fitting and quantification routines.

In 2D J-resolved spectroscopy<sup>15</sup>, the spectral information is spread along two orthogonal axes by adding a step-wise increasing evolution delay in the pulse sequence. This helps improve specificity in the detection of J-coupled metabolites. To further improve detection sensitivity, maximum echo sampling (MES)<sup>16</sup> was introduced for in vivo 2D J-resolved <sup>1</sup>H MRS<sup>8,17</sup>. In the MES scheme, acquisition begins right after the final crusher gradient of the last refocusing pulse in the localization technique. Schulte et al<sup>15</sup> showed that JPRESS with MES had increased sensitivity in comparison to traditional half echo sampling. Yet another advantage of MES is that it adds a tilt to the peak tails in the spectrum<sup>15</sup> and thus largely reduces overlap of the water peak tail with the metabolite peaks of interest.

Another means to clearly distinguish more peaks is ultra-high field (UHF) ( $\geq 7$  T) <sup>1</sup>H MRS<sup>18,19</sup>. It is well known that spectroscopy studies at UHF benefit from both increased spectral resolution and improved SNR in comparison to lower field strengths. However, at UHF  $B_1^+$  inhomogeneity is one of the crucial challenges posed. Also, with increasing static  $B_0$  field strength, chemical shift displacement error between the metabolite peaks increases. Furthermore, quantification for J-coupled peaks such as glucose is easier at a lower field strength as shown previously<sup>20</sup>.

Using simulation and experimental methods at 3 T and 7 T Edden et al<sup>21</sup> demonstrated that the chemical shift displacement effect causes spatially dependent differences in J-evolution of coupled spin systems in JPRESS spectra. Due to the larger spectral dispersion along with reduced peak transmit field strength  $B_1^+$ , the chemical shift displacement error is increasing with increasing field strength. The appearance of additional J-refocused peaks results in loss of intensity in the J-resolved peaks and more spectral overlap thereby leading to uncertain spectral quantification. However, Lin et al<sup>6</sup> compared the spectral quality of JPRESS, J-resolved semiLASER and J-resolved LASER sequences at 3 T and demonstrated that the use of adiabatic pulses reduced the appearance of J-refocused peaks to a great extent due to their higher bandwidth. Adiabatic pulses in the localization schemes are also effective in reducing the effect of  $B_1^+$  inhomogeneity at UHF<sup>22</sup>. Both the implications discussed above emphasize the need to use adiabatic localization when implementing J-resolved spectroscopy at UHF.

Finally, the metabolite cycling (MC) scheme<sup>23</sup> enables simultaneous acquisition of water and metabolite signals. It has been shown for 1D MRS at 3T<sup>24-26</sup>, 7T<sup>27</sup> and 9.4T<sup>28</sup> previously that retrospective frequency alignment based on the MC water signal substantially decreases the linewidth of the resulting spectra yielding a complimentary mechanism to enhance the spectral resolution and data consistency.

Therefore, in this work, we developed a 2D J-resolved metabolite-cycled (MC) semiLASER sequence for human brain application at 9.4 T. Implementing MC<sup>23,28</sup> for J-resolved spectroscopy eliminates the need for acquiring a water reference scan for the sake of eddy current correction or frequency alignment which leads to reduction of scan time. An added bonus is that one can also simultaneously measure both upfield and downfield part of the <sup>1</sup>H spectra when employing MC<sup>28,29</sup>.

Even though, the 2D J-resolved semiLASER acquisition method was developed earlier at 3 T<sup>6</sup>, metabolite quantification was not performed. This work includes basis set simulation for 2D J-resolved semiLASER for the first time. In addition, spectral fitting of 2D spectra (considering 8 and 2 averages per TE) was performed using ProFit v2.0<sup>30</sup>, a dedicated 2D fitting software, which incorporates the theory of LCModel<sup>31</sup> and VARPRO<sup>32</sup> in attaining a global minimum. Fuchs et al<sup>23</sup> enhanced the software by adding a macromolecular model, a spline baseline fit and a spline lineshape model using self-deconvolution. Spectra were considered with 8 and 2 averages per TE for processing, fitting and quantification in order to evaluate if there is significant difference in the concentration values between the low field standard and the accelerated acquisition scheme at UHF.

Subsequently, quantification of metabolites was performed using the internal water referencing method<sup>33</sup> taking into account the tissue composition in the voxel of interest, and water concentration. Finally, quantification results obtained with 2D J-resolved spectroscopy were compared against metabolite concentrations published in previous 1D MRS studies. To the best of our knowledge, the effect of bringing together the two complementary approaches of UHF and 2D J-resolved spectroscopy to enhance spectral resolution on spectral quantification has not been investigated yet. This work is an extension of the initial results reported earlier in a conference abstract<sup>34</sup>.

## 2. Methods

### 2.1 Study Design

All measurements were performed on a 9.4 T Siemens Magnetom whole-body MRI scanner (Siemens Healthineers, Erlangen, Germany) using a home-built coil<sup>35</sup> with eight transmit and sixteen receive channels. Eleven healthy volunteers (6 male and 5 female, age: 28.0 ± 2.3 years) participated in this study. Five volunteers returned for a second visit for the acquisition of 2D MM signal. The study was approved by the local ethics board, and written informed consent was provided by the volunteers prior to the measurements.

### 2.2 MRS Sequence

Figure 1a shows the J-resolved metabolite-cycled (MC) semiLASER sequence diagram. The asymmetric adiabatic MC<sup>28</sup> pulse (duration: 22.4 ms) preceded the conventional semiLASER<sup>28,36</sup> block. A hamming filtered 90 degree-sinc pulse<sup>28</sup> (bandwidth: 8000 Hz) was used for excitation. This pulse was followed by two pairs of adiabatic full passage pulses (duration: 3.5 ms, bandwidth: 8000 Hz). The indirect dimension ( $t_1$ ) was created by inserting an incrementally increasing time delay of  $\Delta t/2$  between the last pair of adiabatic full passage pulses<sup>28</sup>, which encodes the J-evolution. The acquisition of the signal began immediately after the final crusher gradient of the last adiabatic full passage pulse which is called maximum echo sampling (MES) scheme<sup>15</sup>.

In order to optimize the number of TE steps  $n$ , knowledge of  $T_2$  relaxation times of metabolites in vivo at 9.4 T was utilized from Murali-Manohar et al<sup>37</sup> (further explained in section 4.1). Additionally, phantom measurements (Figure 2) were performed with different time increment steps ( $\Delta t$ : 2, 3, and 4 ms) and different number of TE steps ( $n$ : 50, 85) to confirm the absence of J-refocused peaks and whether the peaks are distinctly J-resolved without noise and truncation artifacts in the indirect dimension.

A double inversion recovery (DIR) block preceding the J-resolved MC semiLASER sequence (Figure 1b) was used for the acquisition of macromolecular signal ( $n$ : 60). The inversion pulse<sup>38</sup> duration was 15 ms and the inversion bandwidth was approximately 1650 Hz.

## **2.3 Data Acquisition**

### **2.3.1 Anatomical Imaging**

MP2RAGE<sup>39</sup> images (resolution:  $0.6 \times 0.6 \times 0.6 \text{ mm}^3$ ) were acquired while using the coil in volume mode driving power to all the eight transmit coil elements.

For the MM acquisition, only 2D FLASH images were acquired which then were co-registered to the previously acquired MP2RAGE images using rigid body transformation.

### **2.3.2 Spectroscopy Measurements**

Following the anatomical scan, the volunteer was instructed to remain stationary on the patient table while the coil setup was changed to suit the spectroscopy measurements. Power was driven to the bottom three coil elements near the region of interest using unbalanced three-way Wilkinson splitter<sup>28</sup>. A localizer was reacquired to ensure there was no motion of the volunteer between the anatomical and the spectroscopy scan. This was followed by acquisition of high-resolution 2D FLASH images (in-plane resolution:  $0.7 \times 0.7 \text{ mm}^2$ , slice thickness: 3.5 mm, 25 slices) in the sagittal and transversal orientations to position the spectroscopy voxel ( $2 \times 2 \times 2 \text{ cm}^3$ ) in the occipital lobe. Localized second-order shimming was performed using FAST(EST)MAP<sup>40</sup> setting the shim volume to be 150% of the volume of the voxel of interest. Then, voxel-based power optimization<sup>41,42</sup> was performed on each subject to ensure that the adiabatic conditions were fulfilled.

Two-dimensional metabolite spectra were acquired using the J-resolved MC semiLASER sequence (Figure 1) (TR: 6000 ms, averages per TE step: 8, four-step phase cycling, transmit reference frequency: 2.4 ppm) described above in the MRS sequence section. The MC pulse had a duration of 22.4 ms, frequency factor 2 and offset frequency  $\pm 350 \text{ Hz}$ <sup>28</sup>. TE ranged from 24 to 194 ms ( $n$ : 85) incremented in steps of  $\Delta t = 2 \text{ ms}$ . In addition, 2D water reference signals were acquired (average per TE step: 1, transmit reference frequency: 4.7 ppm) for validation purpose to avoid any saturation effect of the water due to the MC pulse for the quantitative evaluation. The transmit reference frequency for the water reference sequence was set to 4.7 ppm.

In order to account for the MM contribution in the 2D metabolite spectra, 2D MM spectra were acquired from five healthy volunteers using the DIR sequence. The optimized inversion times<sup>30,35</sup> ( $T_{I1}/T_{I2}$ ) combination of 2360 and 625 ms was used in the DIR block as shown in Figure 1b. TE ranged from 24 to 144 ms ( $n$ : 60) since MM signal decays faster in comparison to metabolite signal<sup>29</sup> and 16 averages were acquired at each TE step. All the other acquisition parameters were identical to the metabolite spectra except the TR which was set to 8000 ms<sup>43</sup> to fulfill SAR constraints.

## **2.4 Data Preprocessing**

Spectroscopy raw data were preprocessed using an in-house MATLAB (version 2016a, MathWorks, Natick, MA) tool. Both metabolite and MM data were reconstructed as described in Giapitzakis et al<sup>28</sup>. Firstly, the data were frequency and phase-aligned based on the water signal in the time domain for 85 and 60 blocks for metabolite and MM data respectively. This was followed by metabolite-cycling subtraction and then the data were averaged within each TE block considering 8 and 2 averages per TE. Then Eddy current correction was performed using the phase information from the MC water signal. Signals from all 16 receive channels were then combined using the SVD method. The metabolite and MM data were truncated at 250 and 150 ms respectively for better SNR and considering their  $T_2$  relaxation times at 9.4 T. Automated zeroth- and first-order phase corrections were performed in the J-resolved spectroscopy preprocessing tool<sup>15,36</sup> which is a part of ProFit. The applied phase correction was visually verified for correctness as recommended by the recent consensus article<sup>37</sup>. Using the same ProFit preprocessing tool, residual water in both the dimensions in the spectra was removed using a HSVD method. The final 2D spectrum displayed is after applying Fourier transformation to the data in both the dimensions. SNR of the NAA(CH<sub>3</sub>) peak at 2.008 ppm was calculated as the peak intensity from the real part of the spectrum with respect to the noise window from -4.0 to -1.0 ppm.

## **2.5 MP2RAGE Segmentation**

The high-resolution MP2RAGE images were segmented into gray matter (GM), white matter (WM) and cerebrospinal fluid (CSF) fractions using SPM12<sup>38</sup>. 2D FLASH images acquired during the MM scan session were co-registered to the MP2RAGE images acquired during the first scan session for four volunteers. A home-built Python (v3.7) tool was used to determine the tissue fractions in the voxels of interest.

## **2.6 Spectral Fitting**

Metabolite basis sets corresponding to 85 TE steps were simulated using VesPA (ver. 0.9.3)<sup>44</sup> considering full quantum mechanical density matrix calculations for the semiLASER sequence including the excitation and adiabatic full passage pulse shapes. The simulation also incorporated the sequence timings including the MES scheme. The following metabolites were simulated: n-acetyl aspartate (NAA), NAA glutamate (NAAG),  $\gamma$ -aminobutyric acid (GABA), aspartate (Asp), creatine (Cr), glutamate (Glu), glutamine (Gln), glucose (Glc), glutathione (GSH), glycerophosphocholine (GPC), glycine (Glyc), myo-inositol (ml), scyllo-inositol (Scy), lactate (Lac), phosphocreatine (PCr), phosphocholine (PCho), phosphoethanolamine (PE), and taurine (Tau). Their chemical shifts and coupling constants were chosen according to Govindaraju et al<sup>39</sup>, except for the coupling constant of GABA, for which the values from Near et al<sup>40</sup> were chosen. Subsequently different metabolite peaks were scaled to correct for the number of proton contributions. GPC, PCho and PE combined together is denoted by tCho. Finally, all the 85 1D basis sets and the measured MM spectra were combined to form a complete 2D basis set using an in-house written MATLAB script.

All the metabolite spectra (8 and 2 averages per TE) were fitted using ProFit 2.0<sup>41</sup> (2D PRiOr knowledge FITting). It takes the exponential decay of the metabolite signal and the scalar coupling constants into account and fits the J-resolved spectrum after 2D Fourier transform in both the direct and the indirect dimensions. The non-linear fitting routine iterated four times, each time with increasing degrees of freedom.

## 2.7 Quantification

The formula used for the quantification of metabolites<sup>33</sup> is provided in the Supplementary Material Annex A. Wilcoxon signed rank tests were conducted for each metabolite measurement with 8 averages and 2 averages per TE ( $\alpha/m = 0.003846$ ) and adjusted-p values were calculated.

## 3. Results

### 3.1 Voxel Content and Spectral Quality

The spectra from the phantom tests ( $n: 50$ ,  $\Delta t: 2, 3$ , and  $4$  ms) showed stronger ' $t_1$  ridges'<sup>21</sup> when  $TE_{max}$  was shorter (Figure 2). In other words, when  $TE_{max} = 124$  ms, the ' $t_1$  ridges'<sup>21</sup> were the strongest.  $t_1$  noise was the least when  $TE_{max} = 224$  ms. When  $TE_{max}$  was set to 100, 99, and 100 ms for  $\Delta t: 2$  ms ( $n: 50$ ),  $3$  ms ( $n: 33$ ), and  $4$  ms ( $n: 25$ ) respectively, the ' $t_1$  ridges' were not seen to be impacted (Supplementary figure S1) when changing the delay between TE steps alone. However,  $\Delta t: 2$  ms corresponded to higher SNR since it allows for a greater number of averages for a chosen  $TE_{max}$  and was hence used for all additional experiments since a good SNR is essential for in vivo spectra. Even though the  $t_1$  noise seemed to be minimum for a  $TE_{max} = 224$  ms,  $TE_{max} = 194$  ms was chosen for in vivo studies as  $T_2$  relaxation times are generally longer in phantom than in in vivo tissues.

Figure 3 shows a phantom metabolite spectrum ( $n: 85$ ,  $\Delta t: 2$  ms,  $TE_{max}: 194$  ms) in the magnitude mode. There are neither prominent J-refocused peaks appearing in the spectrum nor are there any visible truncation artifacts or  $t_1$  noise in the indirect dimension.

Figure 4 shows a representative single subject 2D MC J-resolved semiLASER metabolite spectrum ( $n: 85$ ,  $\Delta t: 2$  ms, 8 averages per TE) with an inlay showing the voxel position. Figure 7 shows the respective 2D J-resolved MC semiLASER spectrum considering only 2 averages per TE. The average tissue content of the metabolite spectroscopy measurement voxel in the occipital lobe of eleven healthy volunteers was GM/WM/CSF =  $67 \pm 8 / 29 \pm 9 / 4 \pm 1$  % respectively. The 2D metabolite spectra obtained from voxels in the occipital lobe showed uncoupled peaks lying on the  $f_1 = 0$  Hz axis. This is because during  $t_1$ , only the coupling information is obtained. However, the J-coupled multiplets are resolved at an angle of  $45^\circ$  with respect to  $f_1 = 0$  Hz since  $t_2$  holds both chemical shift and coupling information. The SNR of the NAA(CH<sub>3</sub>) peak in case of 8 averages per TE step was  $906 \pm 147$  and in case of 2 averages per TE step was  $648 \pm 105$  indicating that both the 2-average and the 8-average spectra were of good quality. Also, the spectra did not show any major artifacts such as lipid contamination or water tails. Therefore, no data sets were excluded from further analysis.

The summed MM spectrum from five healthy volunteers is shown in Figure 5.  $M_{0.92}$ ,  $M_{1.21}$ ,  $M_{1.39}$ ,  $M_{1.67}$ ,  $M_{2.04}$ ,  $M_{2.26}$ ,  $M_{2.56}$ ,  $M_{2.70}$ ,  $M_{2.99}$  and  $M_{3.86}$  are clearly seen to have J-resolved peaks. On an average, the MM spectroscopy voxel (five healthy volunteers) had GM/WM/CSF =  $61 \pm 10 / 35 \pm 8 / 4 \pm 3$  % respectively.

### 3.2 Spectral Fitting

A representative metabolite 2D spectral fit is shown in Figure 6. The minimum 2D residual shows good quality fit indicating that the metabolites included in the basis set modeled the acquired data sufficiently well. The fit quality was similar for all the datasets.

### 3.3 Concentrations

Figure 7 shows box plots of concentrations of metabolites calculated in mmol/kg when considering 8 and 2 averages per TE, respectively. The concentration values of the metabolites are calculated from the 2D MRS data both for 8 averages per TE spectra and 2 averages per TE spectra (Table 1).

No significant differences were observed in concentrations of metabolites obtained considering 8 or 2 averages per TE.

## 4. Discussion

### 4.1 Spectral Quality

The phantom tests performed to optimize the step size ( $\Delta t$ ) along with the knowledge of  $T_2$  relaxation times of metabolites in vivo at 9.4 T from Murali-Manohar et al.,<sup>37</sup> led to the choice of  $\Delta t = 2$  ms and number of steps,  $n = 85$  for acquisition in vivo. There was sufficient sampling (500 Hz) in the indirect dimension to cover the frequency range of interest in all cases. The final choice of the scan parameters was made since the appearance of 't<sub>1</sub>-ridges'<sup>21</sup> due to t<sub>1</sub> noise and sinc character from t<sub>1</sub> truncation was diminished significantly by longer TE<sub>max</sub> keeping in mind also comfortable scan durations. Furthermore, T<sub>2</sub>-weighting signal loss was avoided largely by setting the first echo time TE<sub>min</sub> to be 24 ms, as short as possible. According to Murali-Manohar et al.<sup>37</sup>, the T<sub>2</sub> relaxation times in the gray-matter rich voxel present in the occipital lobe ranged from ~45 to 110 ms. Thus, the chosen parameters swept a decent range of TEs from 24 to 194 ms.

Using the adiabatic J-resolved semiLASER localization sequence proposed herein resulted in a chemical shift displacement of 5% per ppm for each voxel dimension (bandwidth: 8000 Hz). Lin et al.<sup>6</sup> showed that the intensity of the J-refocused peaks can be reduced by a factor of

$$\left(1 - \frac{\Delta\delta \cdot B_0}{BW}\right)$$

where  $\Delta\delta$  is the chemical shift difference in ppm of the spins A and X in an AX spin system,  $B_0$  is the frequency of the static magnetic field in MHz and  $BW$  is the bandwidth of the refocusing pulse. Considering lactate coupled peaks at 1.31 and 4.09 ppm, the resulting reduction in the intensity of the J-refocused peaks is 86%. Therefore, there were barely any J-refocused peaks in phantom spectra (Figure 3) and no J-refocused peaks in in vivo spectra (Figure 4) that usually appear because of spatially dependent evolution of the J-coupled peaks<sup>21</sup> due to limited bandwidth refocusing pulses. Consequently, the J-resolved multiplet peaks retained maximum possible intensity.

At 3T typically 8 averages per TE step and 100 TE steps are needed to yield a high quality 2D J-resolved spectrum in about 20 min of measurement time<sup>30</sup>. Hence, 2D J-resolved MC-semiLASER at 9.4T were acquired with 8 averages per TE (acquisition duration of 68 min) and a subset of 2 averages per TE was also investigated (acquisition duration: 17 minutes). It was shown herein that 2 averages per TE (acquisition duration: 17 minutes) yielded the same information as the respective 8 average per TE data set when using metabolite-cycling. Thus, the acquisition time is very similar to 3T 2D J-resolved MRS, which is successfully applied to neuroscientific and clinical studies<sup>8-14</sup>. Considering the high SNR obtained at 9.4T even 1 average per TE would suffice yielding an acquisition duration of only 8 minutes similar to 1D MRS, but in that case a water suppression technique is required instead of employing the 2-step MC method,



which requires at least 2 averages per TE. Even though the TR had to be increased at 9.4 T when compared to 3 T due to SAR, the SNR benefit at UHF allows us to reduce the number of averages in turn bringing down the total acquisition comparable to 2D MRS at 3 T<sup>30</sup> (~17 minutes) or potentially even lower if no MC was implemented (8 minutes).

Altogether, the application of 2D MRS at UHF is thus feasible for clinical and neuroscientific studies. It is known that the additional benefit at 9.4 T comes from the dispersed chemical shift displacement making the peaks overlap less compared to 3 T. This benefit maximizes when using 2D MRS with MES scheme when the overlap of the J-coupling peak is further reduced. This enabled us to detect peaks such as glucose, lactate and glycine, which are not easily visible in 1D MR spectra even from 9.4 T.

In addition to metabolite spectra, 2D J-resolved DIR MC-semiLASER<sup>38,43</sup> (acquisition duration: 128 minutes, averages per TE: 16,  $n$ : 60) sequence was also used to obtain the macromolecular spectra. This MM data was used to account for the underlying MM in the spectral fitting process<sup>47</sup>. MM data was acquired on 5 volunteers.

The knowledge of  $T_2$  relaxation times of MM (approximately ranging from 15 to 37 ms in GM-rich voxel) at 9.4 T from Murali-Manohar et al<sup>37</sup> was utilized in setting  $n = 60$  (covering TE: 24 to 144 ms) for the acquisition of MM spectra using DIR MC J-resolved semiLASER. By  $TE_{max} = 144$  ms, MM signal decayed completely. Therefore, for  $n = 61$  to 85 no corresponding MM spectra were provided in the basis set for metabolite spectral fitting. This study presents a 2D J-resolved MM spectrum (Figure 5) for the first time in vivo in the human brain.  $M_{0.92}$ ,  $M_{1.21}$ ,  $M_{1.39}$ ,  $M_{1.67}$ ,  $M_{1.75}$ ,  $M_{2.04}$ ,  $M_{2.26}$ ,  $M_{2.56}$ ,  $M_{2.70}$ ,  $M_{2.99}$  and  $M_{3.86}$  are observed to undergo J-evolution and they appear as multiplets in the 2D J-resolved spectrum shown in Figure 5 indicating that these peaks have J-coupled spin systems. This observation agrees with Behar et al<sup>45</sup> who reported the above-mentioned peaks (except  $M_{2.56}$  and  $M_{2.70}$ ) as J-coupled MM observed from COSY and J-resolved spectra of dialyzed human cerebral cytosol at 8.4 T. Giapitzakis et al<sup>38</sup> reported  $M_{2.56}$  and  $M_{2.70}$  peaks for the first time and assigned them to  $\beta$ -methylene protons of aspartyl groups which correspond to doublet-of-doublets. This manuscript presents in vivo 2D MM spectra for the first time. Figure 5 also shows  $M_{1.75}$ ,  $M_{1.91}$ ,  $M_{1.95}$ ,  $M_{2.32}$ ,  $M_{2.36}$ ,  $M_{3.02}$ ,  $M_{3.09}$ ,  $M_{3.17}$ , and  $M_{3.28}$  peaks which are observed here in 2D MRS, but not in 1D MRS<sup>37,38,43</sup> in the human brain at 9.4 T. These MM peaks other than  $M_{1.75}$ ,  $M_{2.32}$  and  $M_{3.28}$  were previously only reported at 17.2 T in rat brain by Lopez et al<sup>46</sup>.

Thus, 2D MRS at UHF holds the potential to answer some basic research questions such as assigning unlabeled peaks or in understanding the overlap and J-coupling behavior of the MM peaks.

## **4.2 Spectral Fitting**

Bandwidth of the refocusing pulse was taken into account while simulating the basis sets in VesPA in order to simulate J-refocused peaks if any, as suggested earlier<sup>21</sup>. The basis sets simulated to fit the 2D metabolite spectra using VesPA also included real pulse shapes with exact durations, bandwidths and the MES scheme. It can be seen from Figure 6 that the simulated 2D basis set fits the data very well.

Spectral fitting of 2D J-resolved data using Profit 2.0 can also be used to determine  $T_2$  relaxation times of even low-concentration J-coupled metabolites as shown by Wyss et al<sup>48</sup>, which is the subject of a future study.

### 4.3 Metabolite Concentrations

This study quantifies and reports concentration values of 16 metabolites in mmol/kg using an adiabatic 2D J-resolved localization technique at 9.4T in the human brain for the first time. Concentration values of metabolites calculated while considering 8 and 2 averages per TE for the 2D MRS spectra with no significant differences between the values (Figure 7). The calculated millimolar concentration values lie within the range of values that were reported in previous literature<sup>37,41,49-51</sup> for most of the metabolites. Mekle et al<sup>41</sup> and Deelchand et al<sup>51</sup> did not perform  $T_2$  relaxation correction. However, these studies used shorter TE times; therefore, the contribution from  $T_2$  weighting may have been insignificant. All the studies included experimentally acquired MM spectrum during the fitting procedure. Mekle et al<sup>41</sup> set tCr to 8 mmol/kg and used it as internal reference standard.

For metabolites with J-coupled spin systems, low peak amplitudes and/or overlap with larger singlets such as GABA, GSH, NAAG and Tau the concentrations measured from this study are in line with previous 1D MRS studies at 7T<sup>41,50</sup> and 9.4T<sup>37,49</sup>. Moreover, the 2D MRS technique could quantify Glc and Lac, which are otherwise challenging to quantify. 2D MRS also allowed for the separation of Glycine and ml. Separation of PCr and Cr was achieved in this study along with two previous 9.4T study<sup>37,49</sup> and two previous 7T studies. The concentration of Asp measured in this study is in line with two out of three previous 9.4T<sup>49,51</sup> and two 7T human brain studies<sup>41,50</sup>. Gln concentrations from this study are closely matching those measured in two previous 7T studies<sup>41,50</sup> and one 9.4T study<sup>51</sup>, but deviate from results of two other previous 1D MRS studies at 9.4T<sup>37,49</sup>. Gln concentration estimate from those 1D MRS studies<sup>37,49</sup> is higher than expected. The higher estimation of Gln in the 1D MRS study could come from negative LCModel spline baseline near Gln as pointed out in the respective studies. Fitting of 1D MRS data using recently proposed ProFit-1D<sup>52</sup>, which uses more advanced spline baseline modeling, may help overcome this issue,

### 5. Conclusion

2D J-resolved MC semiLASER was successfully implemented for human brain application at 9.4 T. The development of a dedicated analysis pipeline allowed for quantification of the tissue concentrations of 16 human brain metabolites including those with lower SNR and J-coupling induced multiplet spectral pattern such as GABA, Gln, Lac, and Glc. It was also shown that this information can be obtained in a scan time that allows application to neuroscientific and clinical studies in future. In addition, the 2D resolved macromolecular spectrum allows for the observation of additional peaks  $M_{1.75}$ ,  $M_{1.91}$ ,  $M_{1.95}$ ,  $M_{2.32}$ ,  $M_{2.36}$ ,  $M_{3.02}$ ,  $M_{3.09}$ ,  $M_{3.17}$ , and  $M_{3.28}$  peaks, which are not detectable with 1D MRS even at 9.4T.

### Acknowledgement

The authors would like to thank Brian Soher for providing the Vespa simulation code for semiLASER sequence. Financial support by the Horizon 2020/ CDS-QUAMRI Grant number: 634541 (A. Henning, T. Borbath, and S. Murali-Manohar), SYNAPLAST Grant number: 679927 (A. Henning, A.M. Wright, and S. Murali-Manohar), and Cancer Prevention and Research Institute of Texas (CPRIT) Grant number: RR180056 (A. Henning) are gratefully acknowledged.

### List of Figures:

**Figure 1:** Pulse sequence diagram of J-resolved metabolite-cycled semiLASER localization scheme. The two inversion pulses were turned off when acquiring the metabolite spectra. For the acquisition of macromolecular spectra, double inversion recovery technique was used with  $T_{I1}/T_{I2}$  set to 2360/625 ms. The indirect dimension is created by increasing the time interval between the last two AFP pulses by  $\Delta t/2$ . Both the sequences have maximum echo sampling scheme implemented i.e., acquisition begins right after the final crusher gradient of the last AFP.

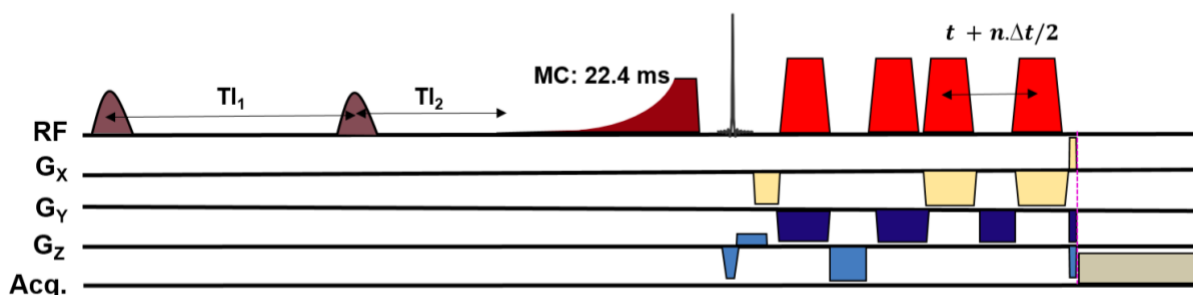


**Figure 2:** (Top to bottom) 2D J-resolved MC semiLASER spectra from Braino phantom containing NAA, Cr, Cho, Glu and Lac with  $n = 50$  and  $\Delta t = 2, 3$  and  $4$  ms. White arrows indicate the  $t_1$ -ridges as a result of  $t_1$  noise and truncation sinc artifacts in the indirect dimension. The ridges are strongly pronounced when  $TE_{max} = 124$  ms and minimum when  $TE_{max} = 224$  ms.

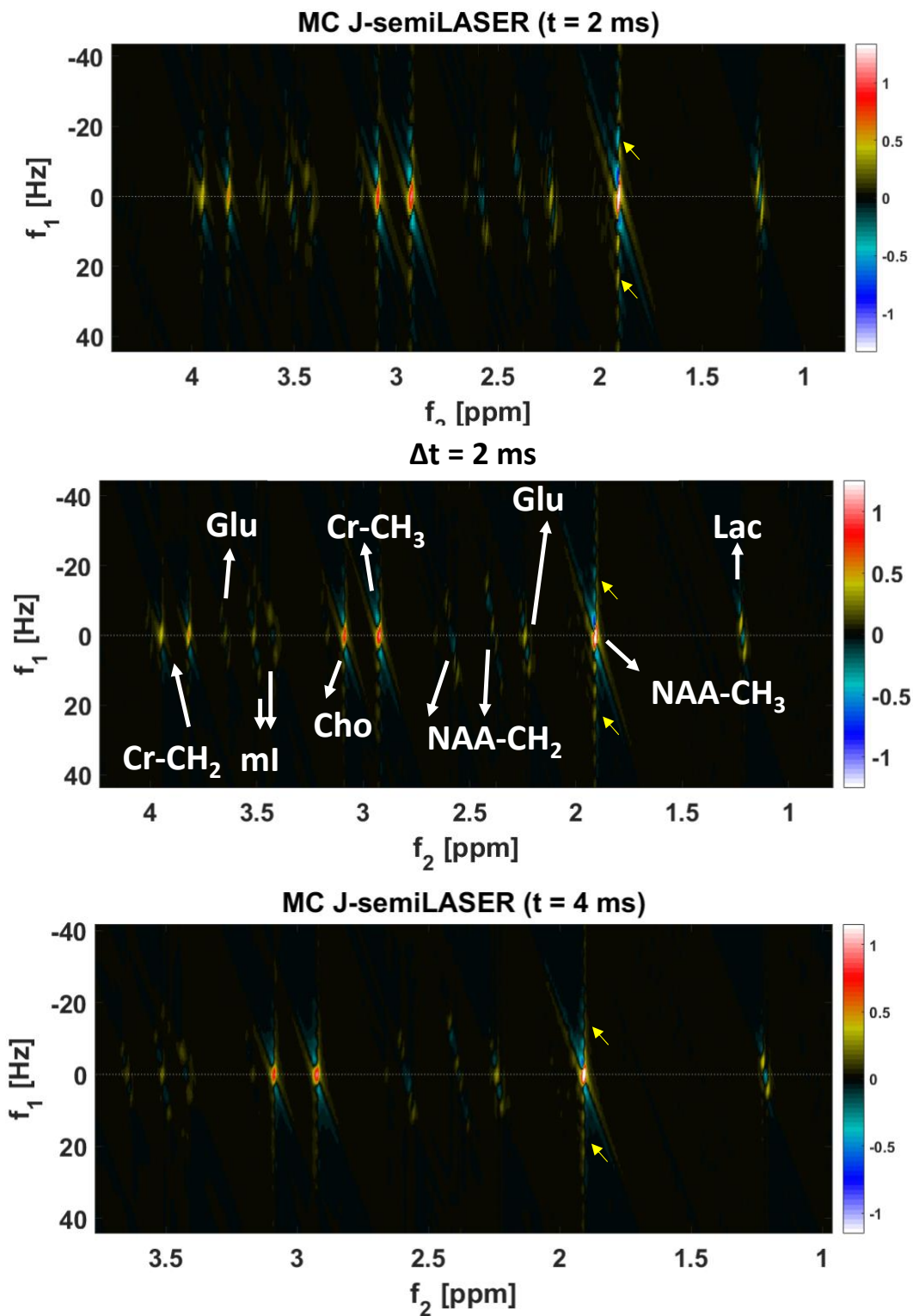


**Figure 3:** a) 2D metabolite spectrum from Braino phantom ( $n = 85$ ,  $\Delta t = 2$ ms) in magnitude mode b) Zoomed in view of the lactate peak showing a J-resolved doublet but barely any J-refocused peaks. An 86% suppression (considering Lac peaks at 1.31 and 4.09 ppm since they have a maximum separation of values in the observable range of the spectrum) of the J-refocused peaks is expected when calculated as suggested by Lin et al<sup>6</sup> resulting in barely any visible J-refocused peaks. This in turn leads to maximum intensity of the J-resolved peaks.

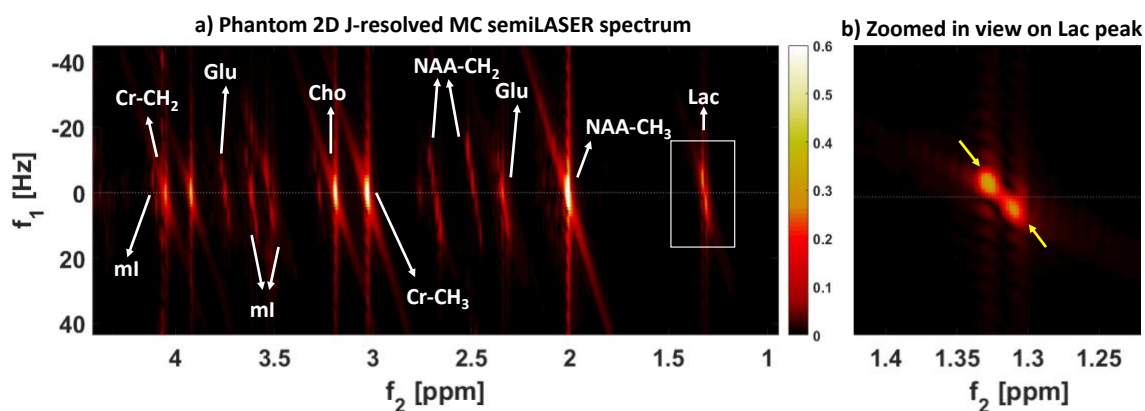


**Figure 4:** 2D J-resolved MC semiLASER spectrum from a representative subject with  $n = 85$  and  $\Delta t = 2$  ms. The figure inlay shows the voxel positioning on the MP2RAGE image in transversal view. Additionally, the observed metabolites are labeled in the figure.

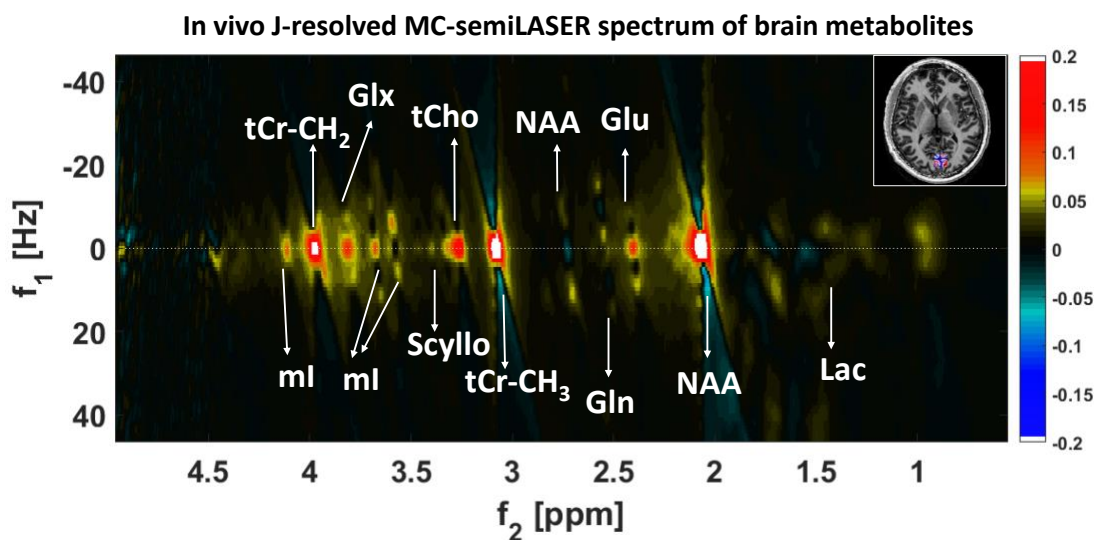


**Figure 5:** 2D DIR J-resolved MC semiLASER ( $T_1/T_2$ : 2360/625 ms,  $n = 60$ ,  $\Delta t = 2$  ms) summed spectrum from five healthy volunteers. The subscripts in the labelled MM peaks are the chemical shift in ppm at which the respective MM resonance occurs.

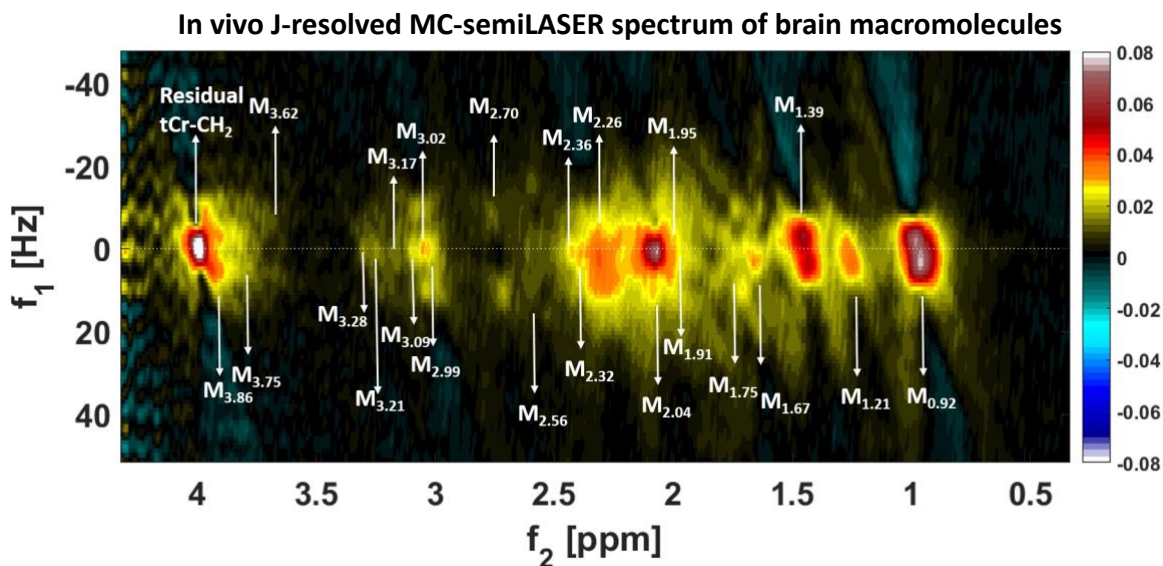


**Figure 6:** A representative fit of 2D J-resolved MC semiLASER data acquired at 9.4 T. The figure shows the data, the fit and the residual from top to bottom scaled similarly. The fitting was performed in ProFit 2.0 using a tailored 2D basis set created using VesPA.

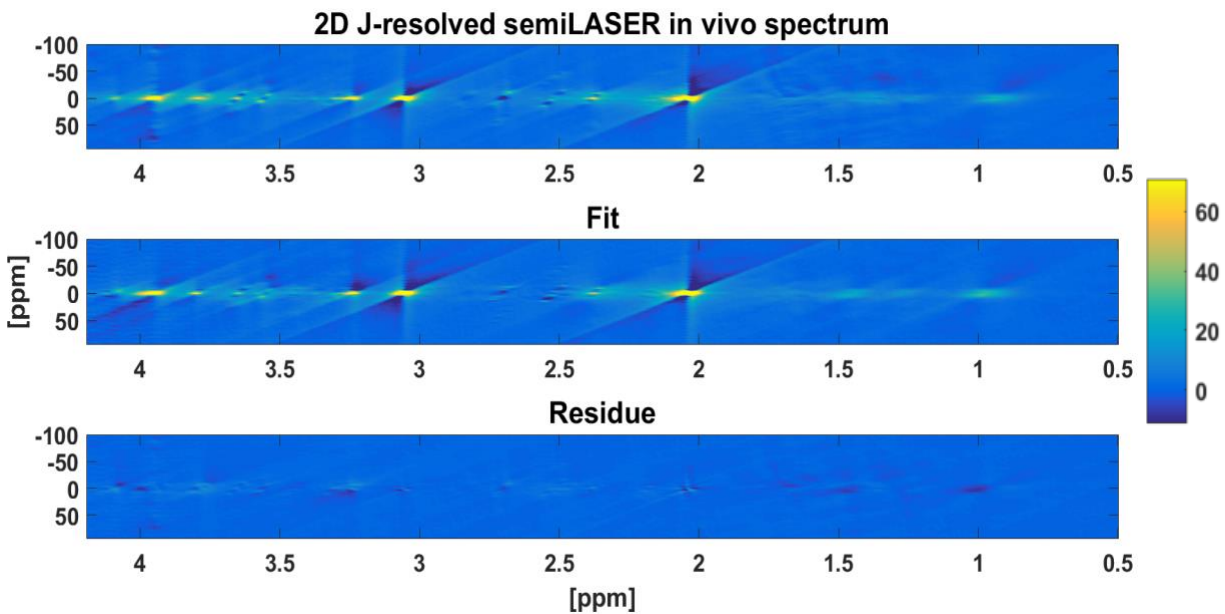


**Figure 7:** Box plots of metabolite concentrations in mmol/kg measured using 2D J-resolved MC semiLASER spectra (with 8 averages and 2 averages per TE). No significant differences were noted observed in concentrations of metabolites obtained considering 8 or 2 averages per TE. Horizontal lines inside the box plots show median values (50% quartile). The bottom and the top boundaries of the boxes indicate 25% and 75% quartiles respectively. Plus signs (+) show outlier values.

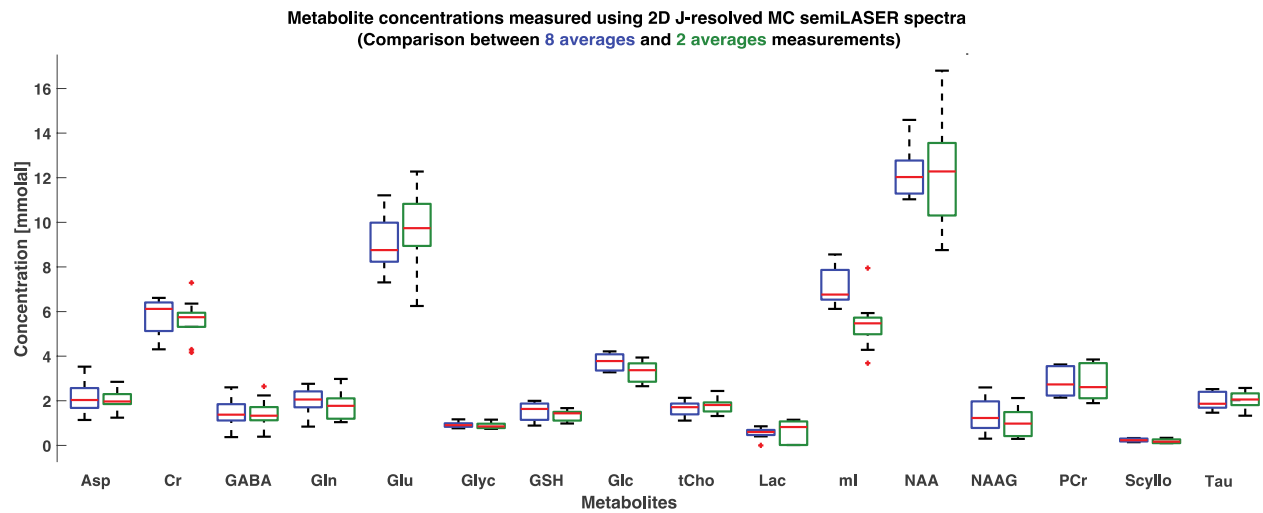


**Table 1:** Comparison of concentration levels of metabolites reported in the study to literature at ultra-high field. Quantification results from this study in mmol/kg are reported for 16 metabolites after correcting for tissue content and water and metabolite relaxation times. ProFit2.0 accounts for the  $T_2$  relaxation effects of the metabolites.  $T_1$  relaxation times at 9.4 T from Wright et al<sup>49</sup> were used to account for the  $T_1$ -weighting of metabolites.

Metabolites	Concentration values [mmol/kg]						
	2D MRS (8 averages per TE) (This work)	2D MRS (2 averages per TE) (This work)	Wright 9.4 T (2021)	Murali- Manohar 9.4 T (2020)	Mekle 7T (2009)	Deelchand 9.4T (2010)	Marjanska 7T (2012)
Asp	2.13 ± 0.64	1.96 ± 0.48	4.3 ± 0.5	4.84 ± 1.15	2.9 ± 0.5	2.1 ± 0.5	2.9 ± 0.8
Cr	5.77 ± 0.80	5.59 ± 0.92	-	5.7 ± 0.85	5 ± 0.3	3.2 ± 0.5	-
GABA	1.37 ± 0.62	1.40 ± 0.66	1.2 ± 0.8	1.87 ± 0.92	1.3 ± 0.15	1.3 ± 0.4	1.5 ± 0.3
Glc	1.65 ± 0.33	1.75 ± 0.32	-	-	-	-	-
Gln	1.96 ± 0.59	1.74 ± 0.60	7.9 ± 1.0	7.61 ± 0.91	2.2 ± 0.4	2.2 ± 0.2	1.5 ± 0.5
Glu	9.11 ± 1.21	9.57 ± 1.75	12.1 ± 1.3	10.9 ± 0.8	9.9 ± 0.9	9.3 ± 0.9	9.6 ± 1.3
Glyc	0.93 ± 0.11	0.86 ± 0.13	0.9 ± 0.2	1.11 ± 0.28	-	-	0.7 ± 0.1
GSH	1.51 ± 0.39	1.34 ± 0.24	1.5 ± 0.3	1.72 ± 0.16	1.3 ± 0.2	1.1 ± 0.3	1.1 ± 0.1
Lac	0.55 ± 0.22	0.63 ± 0.18	-	-	0.7 ± 0.1	0.5 ± 0.1	0.8 ± 0.2
ml	7.05 ± 0.79	5.42 ± 1.12	5.5 ± 0.7	5.22 ± 0.45	5.7 ± 0.5	5.3 ± 0.4	6.4 ± 0.8
NAA	12.20 ± 1.03	12.11 ± 2.33	11.9 ± 0.8	12.61 ± 1.02	11.8 ± 0.2	13.5 ± 1.6	12.6 ± 1.7
NAAG	1.35 ± 0.73	0.99 ± 0.62	1.7 ± 0.3	1.42 ± 0.19	1.1 ± 0.4	1.1 ± 0.5	0.4 ± 0.2
PCr	2.86 ± 0.61	2.79 ± 0.78	-	4.43 ± 0.83	2.2 ± 0.19	3 ± 0.3	-
Scyllo	0.24 ± 0.06	0.17 ± 0.89	0.2 ± 0.1	0.13 ± 0.06	0.3 ± 0.12	0.3 ± 0.2	0.4 ± 0.1
Tau	1.96 ± 0.37	2.0 ± 0.41	1.7 ± 0.5	1.58 ± 0.37	1.5 ± 0.3	1.3 ± 0.2	2.1 ± 0.3
tCho	3.75 ± 0.38	3.35 ± 0.27	2.9 ± 0.8	3.31 ± 0.95	3.6 ± 0.3	2.5 ± 0.5	-
tCr	8.64 ± 1.03	9.18 ± 1.44	9.5 ± 1.0	10.10 ± 0.46	8.0 ± 0.4	7.7 ± 0.4	8.7 ± 1.1

## Supplementary figure captions

**Supplementary figure S1:** (Top to bottom) Phantom spectrum with  $TE_{max} = 100, 99,$  and  $100$  ms for  $\Delta t$ : 2 ms ( $n$ : 50), 3 ms ( $n$ : 33), and 4 ms ( $n$ : 25) respectively. SNR is higher when  $\Delta t$ : 2 ms compared to 3 and 4 ms;  $t_1$  ridges are not seen to be impacted.

**Supplementary figure S2:** Two-dimensional J-resolved MC semiLASER spectrum in magnitude mode from a representative subject. This spectrum was created considering 2 averages per TE (scan duration: 17 minutes).

## References

1. Öz G, Alger JR, Barker PB, et al. Clinical proton MR spectroscopy in central nervous system disorders. *Radiology*. 2014;270(3):658-679.
2. Stanley JA, Pettegrew JW, Keshavan MS. Magnetic resonance spectroscopy in schizophrenia: methodological issues and findings—part I. *Biological psychiatry*. 2000;48(5):357-368.
3. Aue W, Bartholdi E, Ernst RR. Two-dimensional spectroscopy. Application to nuclear magnetic resonance. *The Journal of Chemical Physics*. 1976;64(5):2229-2246.



4. Macura S, Ernst R. Elucidation of cross relaxation in liquids by two-dimensional NMR spectroscopy. *Molecular Physics*. 1980;41(1):95-117.
5. Ryner LN, Sorenson JA, Thomas MA. Localized 2D J-resolved <sup>1</sup>H MR spectroscopy: strong coupling effects in vitro and in vivo. *Magnetic resonance imaging*. 1995;13(6):853-869.
6. Lin M, Kumar A, Yang S. Two-dimensional J-resolved LASER and semi-LASER spectroscopy of human brain. *Magnetic resonance in medicine*. 2014;71(3):911-920.
7. Thomas MA, Hattori N, Umeda M, Sawada T, Naruse S. Evaluation of two-dimensional L-COSY and JPRESS using a 3 T MRI scanner: from phantoms to human brain in vivo. *NMR in Biomedicine: An International Journal Devoted to the Development and Application of Magnetic Resonance In Vivo*. 2003;16(5):245-251.
8. Kotitschke K, Jung H, Nekolla S, Haase A, Bauer A, Bogdahn U. High-resolution one- and two-dimensional <sup>1</sup>H MRS of human brain tumor and normal glial cells. *NMR in Biomedicine*. 1994;7(3):111-120.
9. Ke Y, Cohen BM, Bang JY, Yang M, Renshaw PF. Assessment of GABA concentration in human brain using two-dimensional proton magnetic resonance spectroscopy. *Psychiatry Research: Neuroimaging*. 2000;100(3):169-178.
10. Rémy C, Grand S, Laï ES, et al. <sup>1</sup>H MRS of human brain abscesses in vivo and in vitro. *Magnetic resonance in medicine*. 1995;34(4):508-514.
11. Jensen JE, deB. Frederick B, Renshaw PF. Grey and white matter GABA level differences in the human brain using two-dimensional, J-resolved spectroscopic imaging. *NMR in Biomedicine: An International Journal Devoted to the Development and Application of Magnetic Resonance In vivo*. 2005;18(8):570-576.
12. Walter M, Henning A, Grimm S, et al. The relationship between aberrant neuronal activation in the pregenual anterior cingulate, altered glutamatergic metabolism, and anhedonia in major depression. *Archives of general psychiatry*. 2009;66(5):478-486.
13. Soeiro-de-Souza MG, Pastorello BF, Leite CdC, Henning A, Moreno RA, Garcia Otaduy MC. Dorsal anterior cingulate lactate and glutathione levels in euthymic bipolar I disorder: <sup>1</sup>H-MRS study. *International Journal of Neuropsychopharmacology*. 2016;19(8):pyw032.
14. Ramadan S, Lin A, Stanwell P. Glutamate and glutamine: a review of in vivo MRS in the human brain. *NMR in Biomedicine*. 2013;26(12):1630-1646.
15. Schulte RF, Lange T, Beck J, Meier D, Boesiger P. Improved two-dimensional J-resolved spectroscopy. *NMR in Biomedicine: An International Journal Devoted to the Development and Application of Magnetic Resonance In vivo*. 2006;19(2):264-270.
16. Macura S, Brown LR. Improved sensitivity and resolution in two-dimensional homonuclear J-resolved NMR spectroscopy of macromolecules. *Journal of Magnetic Resonance (1969)*. 1983;53(3):529-535.
17. Kühn B, Dreher W, Leibfritz D, Heller M. Homonuclear uncoupled <sup>1</sup>H-spectroscopy of the human brain using weighted accumulation schemes. *Magnetic resonance imaging*. 1999;17(8):1193-1201.
18. Ladd ME, Bachert P, Meyerspeer M, et al. Pros and cons of ultra-high-field MRI/MRS for human application. *Progress in nuclear magnetic resonance spectroscopy*. 2018;109:1-50.
19. Henning A. Proton and multinuclear magnetic resonance spectroscopy in the human brain at ultra-high field strength: A review. *Neuroimage*. 2018;168:181-198.
20. Park YD, D; Joers, J; Kumar, A; Alvear A; Moheet, A; Seaquist, E; Öz, G. Comparison of neurochemical quantification at 3T vs 7T with an advanced MRS protocol under the same physiological status. *Annual meeting of International Society for Magnetic Resonance in Medicine*. 2024.

21. Edden RA, Barker PB. If J doesn't evolve, it won't J-resolve: J-PRESS with bandwidth-limited refocusing pulses. *Magnetic resonance in medicine*. 2011;65(6):1509-1514.
22. De Graaf RA. *In vivo NMR spectroscopy: principles and techniques*. John Wiley & Sons; 2019.
23. Dreher W, Leibfritz D. New method for the simultaneous detection of metabolites and water in localized in vivo 1H nuclear magnetic resonance spectroscopy. *Magnetic Resonance in Medicine: An Official Journal of the International Society for Magnetic Resonance in Medicine*. 2005;54(1):190-195.
24. Chan KL, Hock A, Edden RA, MacMillan EL, Henning A. Improved prospective frequency correction for macromolecule-suppressed GABA editing with metabolite cycling at 3T. *Magnetic resonance in medicine*. 2021;86(6):2945-2956.
25. Fillmer A, Hock A, Cameron D, Henning A. Non-water-suppressed 1H MR spectroscopy with orientational prior knowledge shows potential for separating intra-and extramyocellular lipid signals in human myocardium. *Scientific reports*. 2017;7(1):16898.
26. Hock A, MacMillan EL, Fuchs A, et al. Non-water-suppressed proton MR spectroscopy improves spectral quality in the human spinal cord. *Magnetic resonance in medicine*. 2013;69(5):1253-1260.
27. Xavier A, Arteaga de Castro C, Andia ME, et al. Metabolite cycled liver 1H MRS on a 7 T parallel transmit system. *NMR in Biomedicine*. 2020;33(8):e4343.
28. Giapitzakis IA, Shao T, Avdievich N, Mekle R, Kreis R, Henning A. Metabolite-cycled STEAM and semi-LASER localization for MR spectroscopy of the human brain at 9.4 T. *Magnetic resonance in medicine*. 2018;79(4):1841-1850.
29. MacMillan EL, Chong DG, Dreher W, Henning A, Boesch C, Kreis R. Magnetization exchange with water and T1 relaxation of the downfield resonances in human brain spectra at 3.0 T. *Magnetic resonance in medicine*. 2011;65(5):1239-1246.
30. Fuchs A, Boesiger P, Schulte RF, Henning A. ProFit revisited. *Magnetic Resonance in Medicine*. 2014;71(2):458-468.
31. Provencher SW. Estimation of metabolite concentrations from localized in vivo proton NMR spectra. *Magnetic resonance in medicine*. 1993;30(6):672-679.
32. Van der Veen J, De Beer R, Luyten P, Van Ormondt D. Accurate quantification of in vivo 31P NMR signals using the variable projection method and prior knowledge. *Magnetic Resonance in Medicine*. 1988;6(1):92-98.
33. Gasparovic C, Song T, Devier D, et al. Use of tissue water as a concentration reference for proton spectroscopic imaging. *Magnetic Resonance in Medicine: An Official Journal of the International Society for Magnetic Resonance in Medicine*. 2006;55(6):1219-1226.
34. Murali-Manohar S, Borbath T, Wright AM, Henning A. Quantification of human brain metabolites using two-dimensional J-resolved metabolite-cycled semiLASER at 9.4 T. 2021.
35. Avdievich NI, Giapitzakis IA, Pfrommer A, Henning A. Decoupling of a tight-fit transceiver phased array for human brain imaging at 9.4 T: Loop overlapping rediscovered. *Magnetic resonance in medicine*. 2018;79(2):1200-1211.
36. Scheenen TW, Klomp DW, Wijnen JP, Heerschap A. Short echo time 1H-MRSI of the human brain at 3T with minimal chemical shift displacement errors using adiabatic refocusing pulses. *Magnetic Resonance in Medicine: An Official Journal of the International Society for Magnetic Resonance in Medicine*. 2008;59(1):1-6.
37. Murali-Manohar S, Borbath T, Wright AM, Soher B, Mekle R, Henning A. T2 relaxation times of macromolecules and metabolites in the human brain at 9.4 T. *Magnetic resonance in medicine*. 2020;84(2):542-558.
38. Giapitzakis IA, Avdievich N, Henning A. Characterization of macromolecular baseline of human brain using metabolite cycled semi-LASER at 9.4 T. *Magnetic resonance in medicine*. 2018;80(2):462-473.

39. Hagberg GE, Bause J, Ethofer T, et al. Whole brain MP2RAGE-based mapping of the longitudinal relaxation time at 9.4 T. *Neuroimage*. 2017;144:203-216.
40. Gruetter R, Tkáč I. Field mapping without reference scan using asymmetric echo-planar techniques. *Magnetic Resonance in Medicine: An Official Journal of the International Society for Magnetic Resonance in Medicine*. 2000;43(2):319-323.
41. Mekle R, Mlynárik V, Gambarota G, Hergt M, Krueger G, Gruetter R. MR spectroscopy of the human brain with enhanced signal intensity at ultrashort echo times on a clinical platform at 3T and 7T. *Magnetic Resonance in Medicine: An Official Journal of the International Society for Magnetic Resonance in Medicine*. 2009;61(6):1279-1285.
42. Versluis MJ, Kan HE, van Buchem MA, Webb AG. Improved signal to noise in proton spectroscopy of the human calf muscle at 7 T using localized B1 calibration. *Magnetic Resonance in Medicine: An Official Journal of the International Society for Magnetic Resonance in Medicine*. 2010;63(1):207-211.
43. Murali-Manohar S, Wright AM, Borbath T, Avdievich NI, Henning A. A novel method to measure T1-relaxation times of macromolecules and quantification of the macromolecular resonances. *Magnetic resonance in medicine*. 2021;85(2):601-614.
44. Soher B, Semanchuk P, Todd D, Steinberg J, Young K. VeSPA: integrated applications for RF pulse design, spectral simulation and MRS data analysis In: Proceedings of the 19th Annual Meeting of ISMRM. *Montreal, Quebec, Canada*. 2011;1410.
45. Behar KL, Rothman DL, Spencer DD, Petroff OA. Analysis of macromolecule resonances in 1H NMR spectra of human brain. *Magnetic Resonance in Medicine*. 1994;32(3):294-302.
46. Lopez-Kolkovskiy AL, Mériaux S, Boumezbaur F. Metabolite and macromolecule T1 and T2 relaxation times in the rat brain in vivo at 17.2 T. *Magnetic resonance in medicine*. 2016;75(2):503-514.
47. Giapitzakis IA, Borbath T, Murali-Manohar S, Avdievich N, Henning A. Investigation of the influence of macromolecules and spline baseline in the fitting model of human brain spectra at 9.4 T. *Magnetic resonance in medicine*. 2019;81(2):746-758.
48. Wyss PO, Bianchini C, Scheidegger M, et al. In vivo estimation of transverse relaxation time constant (T2) of 17 human brain metabolites at 3T. *Magnetic resonance in medicine*. 2018;80(2):452-461.
49. Wright AM, Murali-Manohar S, Borbath T, Avdievich NI, Henning A. Relaxation-corrected macromolecular model enables determination of 1H longitudinal T1-relaxation times and concentrations of human brain metabolites at 9.4 T. *Magnetic resonance in medicine*. 2022;87(1):33-49.
50. Marjańska M, Auerbach EJ, Valabrègue R, Van de Moortele PF, Adriany G, Garwood M. Localized 1H NMR spectroscopy in different regions of human brain in vivo at 7 T: T2 relaxation times and concentrations of cerebral metabolites. *NMR in Biomedicine*. 2012;25(2):332-339.
51. Deelchand DK, Van de Moortele P-F, Adriany G, et al. In vivo 1H NMR spectroscopy of the human brain at 9.4 T: initial results. *Journal of Magnetic Resonance*. 2010;206(1):74-80.
52. Borbath T, Murali-Manohar S, Dorst J, Wright AM, Henning A. ProFit-1D—A 1D fitting software and open-source validation data sets. *Magnetic resonance in medicine*. 2021;86(6):2910-2929.